

Optimization of temporal characteristics of supercontinuum generated in tapered air-clad fibers

Serguei M. Kobtsev and Serguei V. Smirnov
Novosibirsk State University, Novosibirsk, Russia

ABSTRACT

Numerical simulations are used to study temporal characteristics of supercontinuum (SC) generated in tapered and photonic crystal fibers. The dependence of SC temporal characteristics on pumping parameters (pulse duration, peak power, and wavelength) is investigated. The correlation between the SC spectrum and temporal structure is studied. This correlation is shown to be caused by fiber dispersion. An easy way to estimate SC pulse duration by spectrum width is proposed. It is shown that using specially designed fibers with flattened dispersion one can obtain shorter SC pulses.

Keywords: Supercontinuum, Tapered fibers, Photonic crystal fibers, Microstructure fibers

1. INTRODUCTION

The phenomenon of supercontinuum (SC) generation consists in the extremely wide broadening of spectrum when the pumping radiation goes through a nonlinear medium. This effect was observed for the first time in 1970,¹ but recently its active studies commenced prompted by the possibility of making optical fibers with predicted dispersion and nonlinear properties (such as Photonic Crystal Fibers and tapered fibers). Despite the fact that the mechanism of SC generation has not been entirely explained yet, this effect has already found a variety of applications such as optical frequency metrology, tomography, laser spectroscopy and others. Significant spectral broadening (up to two octaves and even more at the level of -20 dB²), which characterizes the SC generation phenomenon, offers an opportunity to use it for making wideband and tunable light sources. Presently, there are some obstacles preventing this, such as instability of SC spectrum, dependence of SC spectrum on pumping noise,³ presence of dips in SC spectra generated with femtosecond pumping pulses, and extremely complex temporal structure of SC, which has not been studied yet.

The majority of works dedicated to the phenomenon of SC generation deal with spectral characteristics of continuum. Now the investigations of SC temporal structure, of mechanisms which lead to its formation are in initial stage. Until now there have been no investigations of the dependence of SC temporal characteristics on pumping and fiber parameters. In [4] both spectral and temporal SC characteristics are considered, however the authors propose no explanation of the dependence of time delay on frequency, notwithstanding observations of this dependence both in experiment and in numerical simulations.

In our work we use numerical simulation based on the extended nonlinear Schrödinger equation (NLSE)⁵:

$$\frac{\partial A}{\partial z} = i \sum_{k=2}^{k_{max}} \frac{i^k}{k!} \beta_k \frac{\partial^k A}{\partial t^k} + i\gamma \left(1 + \frac{i}{\omega_0} \frac{\partial}{\partial t} \right) \left(A(z, t) \int_0^\infty R(t') |A(z, t - t')|^2 dt' \right) \quad (1)$$

where $A(z, t)$ — the envelope of electric field, β_k — the k^{th} dispersion coefficient on the pumping frequency ω_0 , and $\gamma = n_2 \omega_0 / (A_{eff} c)$ — the nonlinear coefficient, where $n_2 = 3.2 \cdot 10^{-20} \text{ m}^2/\text{W}$ — the nonlinear refractive index of quartz and A_{eff} — the effective area of the fundamental mode. The kernel $R(t')$ was obtained from experiments referenced in [6]. The Taylor series expansion for the dispersion operator in (1) is carried out up to $k_{max} = 5$.

Further author information: (Send correspondence to Serguei M. Kobtsev)
Serguei M. Kobtsev: E-mail: kobtsev@lab.nsu.ru, Telephone: +7 3832 397224
Serguei V. Smirnov: E-mail: smirsv@ngs.ru, Telephone: +7 3832 397224, Address: Novosibirsk State University, Pirogova Street, 2, Novosibirsk, 630090, Russia

Using the numerical solution of (1) we investigate the dependence of the duration of SC pulses, generated in tapered air-clad fibers with the diameter of 2.3 μm and length of 10 cm, on pumping parameters — input pulse duration, peak power and wavelength. We investigate the correlation between SC temporal structure and its spectrum. We propose an easy way to estimate the SC pulse duration by the spectrum width, which takes into account the fiber dispersion only. We consider the possibility to reduce the SC pulse duration with the help of optical fibers with flattened dispersion.

2. THE DEPENDENCE OF SC PULSE DURATION ON PUMPING PARAMETERS

Numerical simulations of SC generation in tapered fibers with the diameter of 2.3 μm and the length of 10 cm (zero dispersion wavelength $\lambda_{ZD} \approx 753$ nm) at different values of pumping pulse peak power, duration, and wavelength were carried out. Thus, we used sech^2 input pulses with peak power of 0.5, 2.5, 5, 10, 15, and 20 kW, with the duration of 20, 40, 60, 80, 120, and 140 fs and wavelength of 750, 770, 790, 810, 830, and 850 nm. For each of $6 \times 7 \times 6 = 252$ possible combinations of input pulse parameters mentioned above, we solved numerically the equation (1), this allowing us to make a qualitative analysis of the dependence of SC pulse duration on pumping parameters.

Since there are three pumping parameters to vary — wavelength, peak power and pulse duration, the raw results of our numerical simulations look like a 3D array of SC duration values. For visualization of the results we plotted contour graphs of the dependence of SC pulse duration on pumping pulse peak power and duration. These graphs are plotted for each value of pumping wavelength that we have used to carry out the simulations (see Fig. 1). Each graph is plotted in the axes of input peak power (the horizontal axis, numerical values are given in kilowatts) and input pulse duration (the vertical axis, numerical values are given in femtoseconds). Each graph corresponds to its own fixed value of pumping wavelength, which is specified above the graph. To obtain values of SC pulse duration between the mesh points we used a bicubic spline interpolation. The SC pulse duration values were calculated at the level of -50 dB.

Analysing the graphs in Fig. 1, one can notice the following features in the dependence of SC pulse duration on pumping parameters:

1. The SC pulses become longer at higher values of pumping pulse peak power and duration.
2. The SC pulse duration grows almost linearly as one increases the peak power of input pulses (that corresponds to almost equal distance between level lines on the graph).
3. The SC pulse duration grows as one increases the pumping wavelength practically everywhere in the concerned spectral range.
4. The shorter SC pulses can be obtained with the use of lower values of pumping power, but in this case the spectrum broadening is also weak. The duration of the shortest exit pulse is determined by the fiber dispersion only and can be reached when all of the nonlinear effects are negligible. In this case the high-order dispersion plays a dominant role (that is, the third-order dispersion β_3 and the next orders).

The presence of the dependence of SC temporal structure on input pulse parameters enables to optimize SC temporal characteristics by means of pumping parameter adjustment. However that is not the only and the best way of optimization, because as one changes the pumping parameters the SC spectrum changes as well. Our numerical simulations show that reduction of SC pulse duration using lower values of pumping peak power and input pulse duration is accompanied by contraction of SC spectrum width. Thus, it is necessary to find another method, which gives one control over the temporal characteristics of SC leaving the SC spectrum width intact. To formulate such method we have to understand the correlation between the spectral and temporal structures of SC. This is what we will do in the next section.

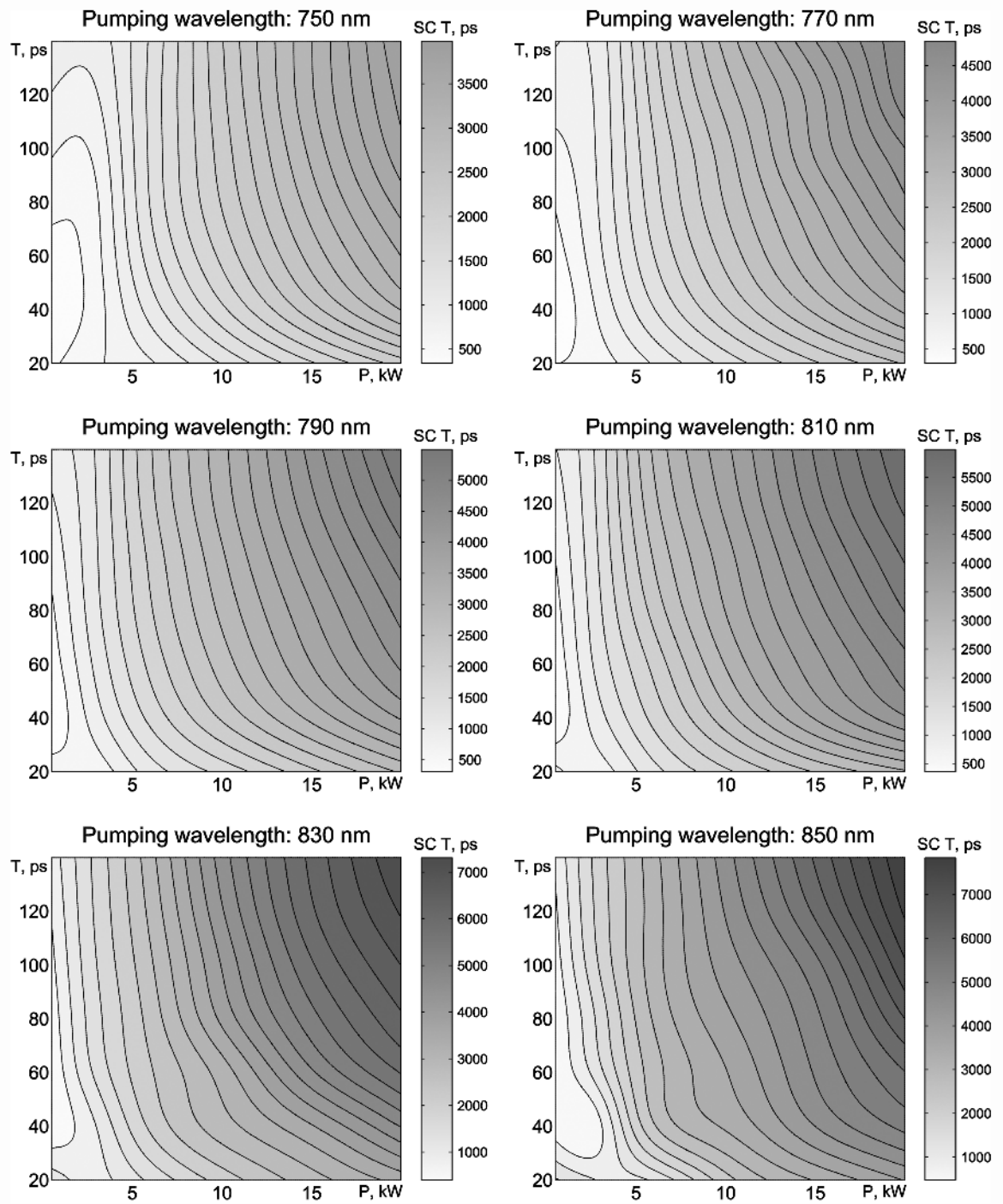


Figure 1. The dependence of SC pulse duration on pumping parameters (wavelength, peak power and duration).

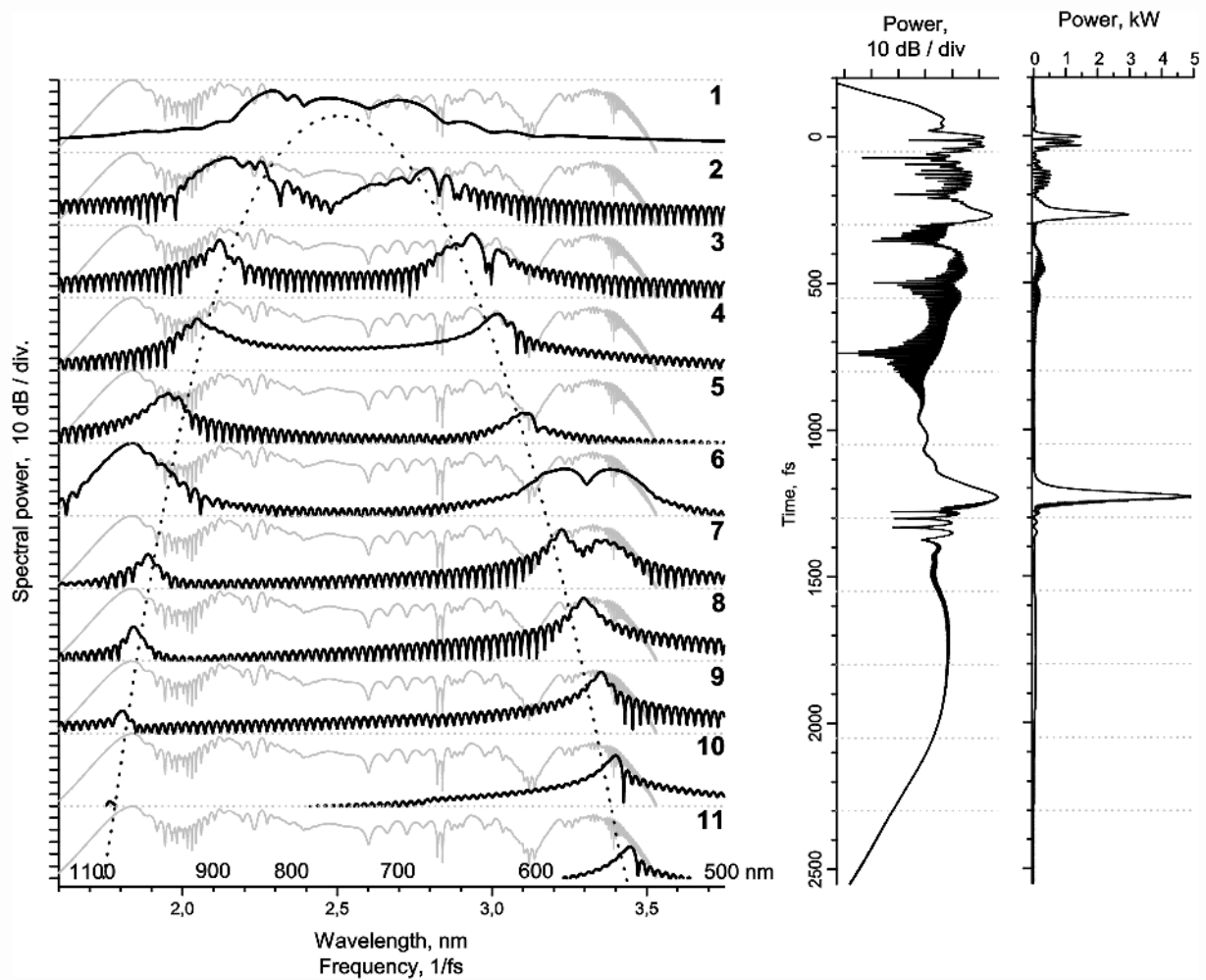


Figure 2. On the left: spectra of SC pulse fragments (shown with a thick line) with the whole SC pulse spectra in the background (shown in grey). The dependence (2) of time delay on frequency caused by fiber group velocity dispersion is shown with dotted line. On the right: SC pulse in time domain with the division into eleven fragments.

3. CORRELATION BETWEEN SC TEMPORAL STRUCTURE AND SPECTRUM

To investigate the correlation between the spectral and temporal structures of SC we used a simulated SC pulse, which was obtained at the output of 10-cm tapered fiber with the diameter of 2.3 mm. The fiber was pumped with sech^2 -pulses with the carrier frequency $\omega_0 = 2.36 \text{ fs}^{-1}$ ($\lambda_0 = 800 \text{ nm}$), peak power of 10 kW and duration at half-height of 40 fs. The SC pulse was divided into eleven time fragments, each of them having a duration of 250 fs (the first fragment contained temporal delays from -200 to 50 fs, the second - from 50 fs to 300 fs, ..., the eleventh - from 2300 fs to 2550 fs). To each of time fragments Fourier transform was applied and the spectrum was plotted in the logarithmic scale of spectral power (see Fig. 2). Each of the SC fragment spectra was plotted over the whole SC pulse spectrum, shown in grey. For convenience the SC pulse graphs in time domain (in linear and logarithmic scales) were placed on the right of the spectra. The scale of time domain graphs was chosen so that each of the time fragments lies opposite to the corresponding spectrum. The pulse fragments are separated with grey dotted lines and there is identical separation between SC fragment spectra shown on the left. The pulse fragments are enumerated from one to eleven following the increase of their temporal coordinate; the numbers are given on the right of the spectra.

Analysing the graphs in Fig. 2 one can see, that the SC radiation is a set of pulses which are separated by

time gaps. These pulses have different frequencies, so a wide spectrum of the whole SC pulse is produced by superposition of relatively narrow spectra of these pulses. Also it is necessary to notice that almost each of SC pulse fragments contains two spectral lines, which are separated by some spectral interval. The width of this interval depends strongly on the time coordinate of the pulse fragment. This relation between the time delay and frequency is caused by the fiber dispersion. The group velocity of a wave packet with carrier frequency ω is $1/\beta_1(\omega)$, where $\beta_1 = \frac{d}{d\omega}\beta(\omega)$. Thus, a wavepacket with central frequency ω changes its time coordinate by

$$\Delta t(\omega) = (\beta_1(\omega) - \beta_1(\omega_0)) \cdot \Delta z \quad (2)$$

while covering the distance Δz along a fiber with the dispersion $\beta(\omega)$. In Fig. 2 the dependence of $\Delta t(\omega)$ with $\Delta z = 10$ cm is shown (the time axis of time domain graph is used to plot this dependence). One can see that the locations of spectral peaks are in agreement with the dotted line, which represents the dependence (2). Against the background of such a good agreement one can see that the spectral peaks of the sixth fragment do not lie on the dotted curve. Indeed, according to the (2) the spectral components of the sixth fragment are to have greater values of time delay. The positions of the spectral peaks of the sixth fragment differ from ones predicted by the fiber dispersion because the sixth fragment contains an optical soliton, which propagates faster than nonsolitonic radiation with the same carrier frequency. Since the speed of the soliton is greater than the group velocity, its time coordinate is less than it is predicted by (2). One can notice that this explanation concerns only the low-frequency part of the sixth fragment spectrum, because the high-frequency part lies in the region of normal fiber dispersion* where solitons can not exist. However the high-frequency part of the spectrum of the sixth fragment is related to the soliton. This nonsolitonic radiation has the same value of group velocity as the soliton propagation velocity, offering a possibility of energy transfer from soliton to the blue-shifted nonsolitonic radiation. This mechanism of SC spectral formation is discussed in^{7,8}, but in these papers the relation between the soliton and high-frequency radiation was shown differently (by means of phase matching).

The results we obtained (the dependence of SC power on time delay, the dependence of SC frequency on time delay and the presence of two frequencies for each value of time delay) are in agreement with recent theoretical and experimental studies by other authors,⁴ but the latter have not shown the relation between the dependence of time delay on frequency and the fiber dispersion.

The expression (2) allows one to make estimation of SC pulse duration by SC spectrum width (with the assumption that there are two frequencies in SC pulse for each value of time delay within the SC pulse duration). The results are presented in Fig. 3. The estimation for SC pulse duration which takes into consideration the fiber dispersion only is shown with solid line. The results of complete numerical simulations, where the fiber dispersion and a whole series of nonlinear optical effects were taken into account, are presented with triangle and round markers (they correspond to different values of pumping pulse duration T_0 : 40 fs for round markers and 100 fs for triangle ones). The maximum discrepancy between the estimation and simulation results shown in fig. 3 amounts to 12%.

4. USE OF FIBERS WITH FLATTENED DISPERSION FOR GENERATION OF ULTRASHORT SC PULSES

Since, as it was shown above, the SC temporal structure is due to fiber dispersion only, it is possible to optimize SC temporal characteristics using optical fibers with special dispersion. In particular, one can use photonic crystal fibers (PCF) with flattened dispersion to produce shorter SC pulses.

There are a lot of works dedicated to design of PCF with flattened dispersion, however the majority of them deal with flattened dispersion near the wavelength of 1500 nm. In our calculations, which were carried out in order to show the possibility to reduce SC pulse duration by use of fibers with flattened dispersion, we used the PCF dispersion, taken from [9]. The effective mode area A_{eff} which appears in (1) was assumed to be equal to the effective area of fundamental mode of tapered fiber with the diameter of 2.3 μm (since no effective mode area was given in [9]). It is necessary to note that using exact value of A_{eff} for the PCF can result in renormalization of pumping peak power only.

*The calculated zero-dispersion wavelength of the fiber is $\lambda_{zD} \approx 753$ nm ($\omega_{zD} \approx 2.5$ fs⁻¹ corresponds to the minimum of the (2), which is plotted in Fig. 2 with a dotted line)

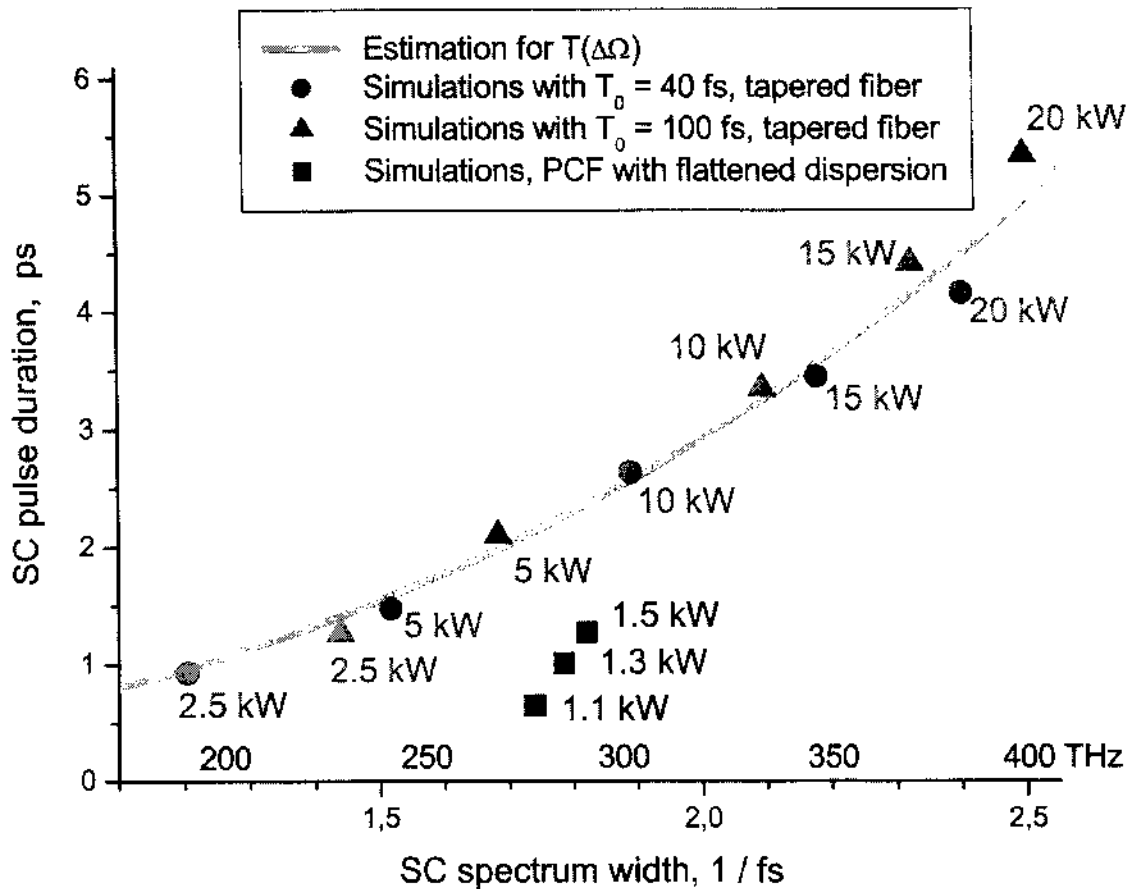


Figure 3. The estimation for SC pulse duration by SC spectrum width (solid line) and the results of complete numerical simulations for tapered fibers and PCF⁹ (markers).

The dependence of the second-order dispersion coefficient β_2 on frequency is shown in Fig. 4 with solid line (for comparison the same dependence for tapered fibers with the diameter of 2.3 μm is shown with dotted line). The results of numerical simulations of SC generation in PCF are presented as a set of points (which are shown with square markers) in the axes of SC pulse duration and SC spectrum width (see Fig. 3). One can see that the duration of SC pulses, generated in PCF with flattened dispersion, is two–three times as short as that of the pulses generated in tapered fibers (the points which correspond to PCF lie under the points which correspond to the tapered fiber in Fig. 3). Thus, the use of PCF with flattened dispersion really allows one to obtain shorter SC pulses. It is relevant to note that for further reduction of SC pulse duration additional investigations are required (first of all to design PCF with much better flattened dispersion).

5. CONCLUSIONS

We explained the dependence of the correlation between SC spectrum and its temporal structure which was observed recently in experiment. The explanation was obtained with the use of the numerical simulations based on extended NLSE. Understanding the correlation between SC temporal structure and spectrum allows us to propose a method to reduce the SC pulse duration with the help of PCF with flattened dispersion. For further optimization of SC temporal characteristics subsequent investigations are required.

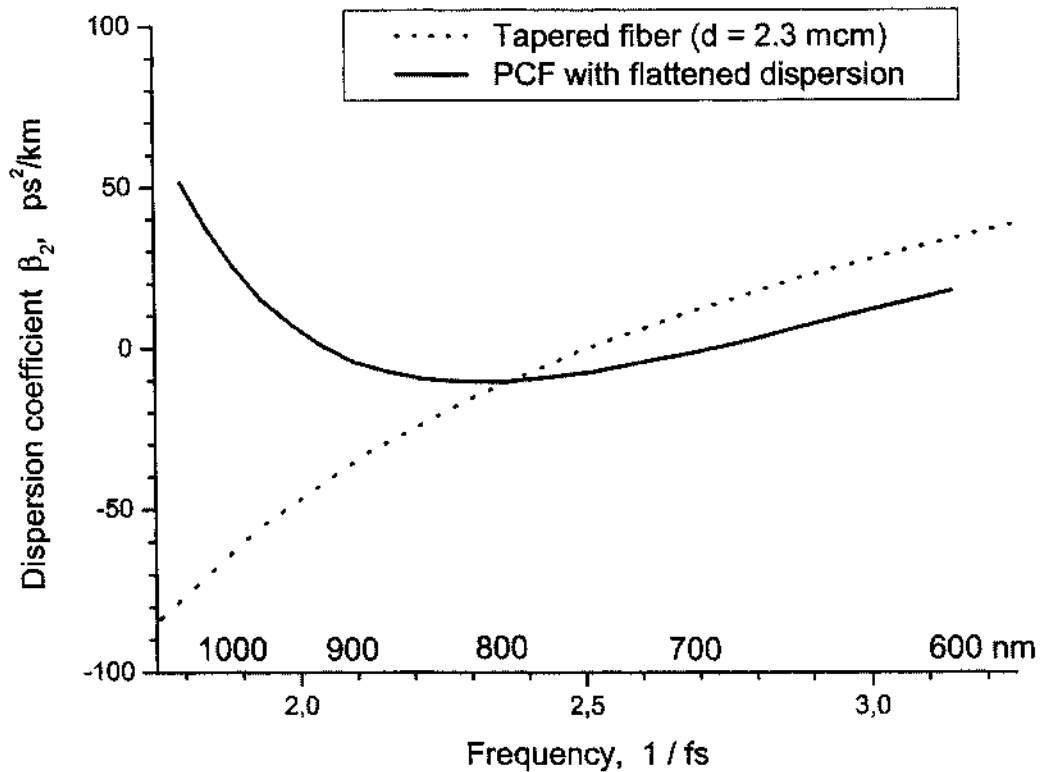


Figure 4. The dependence of the second-order dispersion coefficient β_2 on the frequency for tapered fiber with the diameter of 2.3 μm and PCF.⁹

REFERENCES

1. R. Alfano and S. Shapiro, "Observation of self-phase modulation and small-scale filaments in crystals and glasses," *Phys. Rev. Lett.* **24**, pp. 592–594, 1970.
2. T. Birks, W. Wadsworth, and P. Russel, "Supercontinuum generation in tapered fibers," *Opt. Lett.* **25**, pp. 1415–1417, 2000.
3. K. R. Tamura, H. Kubota, and M. Nakazawa, "Fundamentals of stable continuum generation at high repetition rates," *J. of Quant. El.* **36**, pp. 773–779, 2000.
4. J. M. Dudley, X. Gu, L. Xu, M. Kimmel, E. Zeek, R. T. Patrick O'Shea, S. Coen, and R. S. Windeler, "Cross-correlation frequency resolved optical gating analysis of broadband continuum generation in photonic crystal fiber: simulations and experiments," *Opt. Express* **10**, pp. 1215–1221, 2002.
5. G. P. Agrawal, *Nonlinear Fiber Optics*, Academic Press, 2001.
6. K. J. Blow and D. Wood, "Theoretical description of transient stimulated raman scattering in optical fibers," *J. of Quant. El.* **25**, pp. 2665–2673, 1989.
7. A. Husakou and J. Herrmann, "Supercontinuum generation of higher-order solitons by fission in photonic crystal fibers," *Phys. Rev. Lett.* **87**, p. 203901, 2001.
8. J. Herrmann, U. Griebner, N. Zhavoronkov, A. Husakou, D. Nickel, J. Knight, W. Wadsworth, P. Russel, and G. Korn, "Experimental evidence for supercontinuum generation by fission of higher-order solitons in photonic fibers," *Phys. Rev. Lett.* **88**, p. 173901, 2002.
9. A. Ferrando, E. Silvestre, and P. Andr s, "Designing the properties of dispersion-flattened photonic crystal fibers," *Opt. Express* **9**, pp. 687–697, 2001.